Physics Issues of Compact Drift-Optimized Stellarators

D. A. Spong, S. P. Hirshman, L. A. Berry, J. F. Lyon, R. H. Fowler, D. J. Strickler, M. J. Cole, B. N. Nelson, D. E. Williamson, Oak Ridge National Laboratory, P. O. Box 2009, Oak Ridge, TN 37831-8071, E–mail: spongda@ornl.gov

A. S. Ware, D. Alban, University of Montana, Missoula, MT

R. Sanchez, Universidad Carlos III de Madrid, Madrid, Spain

G. Y. Fu, D. A. Monticello, Princeton Plasma Physics Laboratory, Princeton, NJ

W. H. Miner, Jr., P. M. Valanju, University of Texas, Austin, TX

Abstract

Physics issues are discussed for compact stellarator configurations which achieve good confinement by the fact that the magnetic field modulus, |B|, in magnetic coordinates is dominated by poloidally symmetric components. Two distinct configuration types are considered: (1) those which achieve their drift optimization and rotational transform at low β and low bootstrap current by appropriate plasma shaping; and (2) those which have a greater reliance on plasma β and bootstrap currents for supplying the transform and obtaining quasi–poloidal symmetry. Stability analysis of the latter group of devices against ballooning, kink and vertical displacement modes has indicated that stable <β>'s on the order of 15% are possible. The first class of devices is being considered for a low β near-term experiment that could explore some of the confinement features of the high beta configurations.

1. Introduction

Stellarator optimization techniques have allowed the exploration of design parameters corresponding to compact (aspect ratios in the range $R_0/\langle a\rangle = 2.5 – 4$), low field period ($N_{fp} = 2 – 4$) toroidal devices with attractive physics properties. These configurations permit lower cost near–term experiments with the same plasma minor radius <a> as the more conventional large aspect ratio stellarator approach. In addition, they offer the longer-term potential of a more economically–sized, higher–power density fusion reactor. We have utilized a transport optimization strategy based on quasi-omnegeneity (QO) [1,2] that minimizes particle drifts away from magnetic surfaces. Additional optimization targets are Mercier stability, ballooning stability based on the COBRA [3,4] code, a self-consistent bootstrap current that is reduced (by factors >3) from that in a tokamak, and rotational transform profiles that avoid major resonances.

Previously, [2] we analyzed 3 and 4 field period QO configurations which were close to quasi–helically symmetrical states for aspect ratios in the range of $R_0/\langle a\rangle = 3.5$ - 4. In this paper, we focus on 2 and 3 field period devices that are close to quasi-poloidally symmetrical states for aspect ratios in the range of $R_0/\langle a\rangle = 2.5$ - 3.5. The emergence of this form of quasi–symmetry has been a natural outcome of directing our QO optimization approach toward lower field periods and lower aspect ratio. Quasi-poloidal symmetry offers the unique property of minimizing the viscous damping (i.e., as caused by magnetic pumping) in the direction of the E_r x B drift. This feature may be of importance in accessing enhanced confinement regimes which depend on E_r x B shear and should lead to much lower parallel flows than in quasi-axisymmetric devices [5]. Two configuration choices have emerged from our optimization studies. The first type, which we regard as more appropriate for a near-term

experiment, relies on plasma shaping to achieve most of its rotational transform and quasi-poloidal symmetry. The second type, which we regard as a longer-term option due to its more challenging start-up and heating requirements, derives most of its transform and quasi-symmetry from the finite plasma <β> driven bootstrap currents. In this respect it resembles an advanced tokamak, but because of its quasi-poloidal symmetry the bootstrap current is spatially well aligned and is lower (by factor of 3 or 4) than the equivalent tokamak. This latter feature leads to higher <β> stability toward external kink and vertical modes than in the advanced tokamak.

2. Low <β>, Near Term Experimental Configuration

In Figure 1 we show the flux surface shapes and coils for a 2 field period, $R_0/\langle a \rangle = 2.5$ device which is of the first type mentioned above.

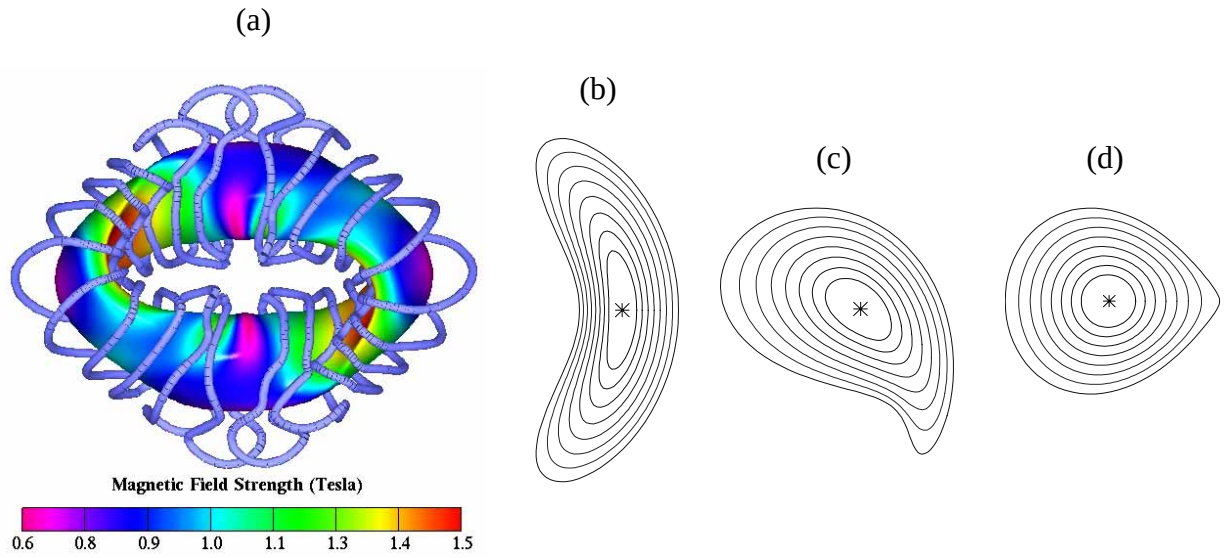

Figure 1. (a) Top view of outer flux surface and modular coils (in blue) for an $N_{fp} = 2$, $R_0/\langle a \rangle = 2.5$ device; (b,c,d) VMEC flux surfaces at toroidal angles $\zeta/N_{fp} = 0°$, 90°, and 180°.

The rotational transform profiles with and without bootstrap current and the Fourier coefficients B_{mn} of |B| are shown in Figures 2(a) and 2(b).

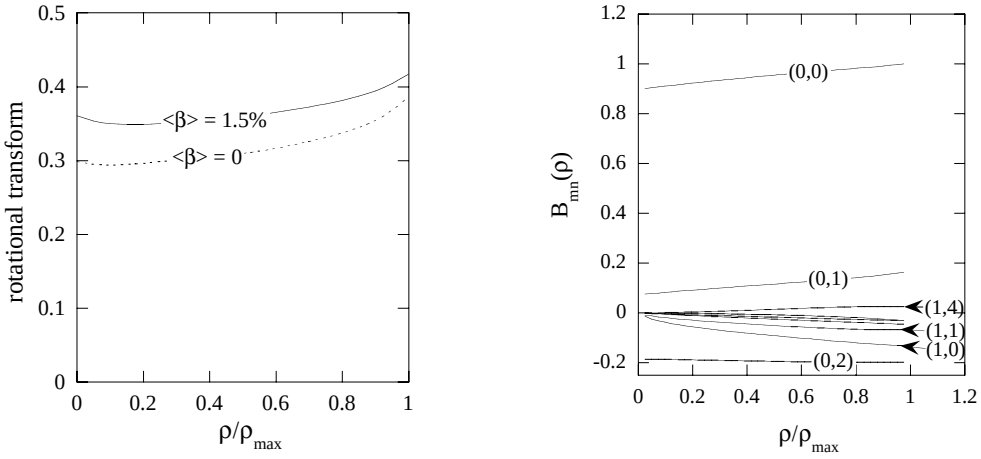

Figure 2 - (a) Rotational transform profiles; and (b) B_{mn} amplitudes vs. toroidal flux - the poloidal and toroidal mode numbers (m,n) are indicated for the larger components of B_{mn}.

As previously indicated, these devices are dominantly quasi-poloidal [i.e., the m = 0 components: (0,0), (0,1), and (0,2) of B_{mn} are the largest] and have most of their rotational transform provided through the external coils. The bootstrap current flows in the direction which increases the transform; this fact, coupled with the positive shear in the transform provides stabilization against neoclassical tearing instabilities. Thresholds for ballooning instabilities are currently found to be $<\beta> = 1.8 - 2\%$. Predicted bootstrap current levels (in the low collisionality limit) for this device are about 1/3 of those in the equivalent tokamak configuration. For example, in a $<B> = 1$ Tesla, $R_0 = 0.8$ meter device at $<\beta> = 1.5\%$, 34 kAmps of bootstrap current would flow, based upon the low collisionality limit.

Our analysis of neoclassical transport in this device has been directed at regimes which would be accessible in a $<B> = 1$ Tesla, $R_0 = 0.8$ meter device with 28 GHz (B = 0.5 T) and 53 GHz (B = 1 T) ECH heating sources available. The impact of supplementary ICH heating (1 MW), which is available in the 40 - 80 MHz range, has also been considered; this would allow access to higher density regimes than ECH (density cutoff limited). Our transport analysis has been carried out with the DELTA5D Monte Carlo model, which is a generalization of an earlier stellarator Monte Carlo code [6] to include energetic beam and alpha populations, ICH heating, global lifetime estimates and bootstrap current options. We assume an ion root ambipolar potential profile which rises from the center inversely with the drop-off in electron temperature profile and take $e\phi/kT_e = 1$ at the plasma edge. We are also developing a self-consistent calculation of the electric field using the DKES model [7] similar to what has been carried out [8] in modeling the W7–AS experiment. Initial results from these calculations near the plasma edge show ion root behavior with $e\phi/kT_e \sim 1$. Table I lists the parameters we have considered for the various heating scenarios (here we assume $Z_{eff} = 1$). We also give the confinement time which results from the Monte Carlo transport model (in column 6) labeled as $\tau_{E,\,global}$ (here $\tau_{E,global}$ is the overall neoclassical energy lifetime, taking into account both $\tau_{E,ion}$ and $\tau_{E,elec}$); in the final column the ISS95 [9] empirical stellarator confinement scaling, assuming no enhancement factor is given for comparison. As can be seen, the neoclassical loss rates are considerably smaller than the ISS95 [9] rates, especially at the higher range of densities that can be accessed with ICRF heating.

Free boundary and field line following calculations have also been carried out based on the modular coil set shown in Figure 1 in order to check that a good reconstruction of flux surfaces is obtained and that neoclassical confinement is preserved. Comparisons of Monte Carlo energy lifetimes based on free boundary equilibria show less than 10% change from the

TABLE I - PLASMA PARAMETERS AND PREDICTED NEOCLASSICAL LIFETIMES FOR A $<B> = 0.5$ TO 1 TESLA, $R_0 = 0.83$ METER, $N_{fp} = 2$, DEVICE, BASED ON ISS95 SCALING WITH ENHANCEMENT FACTOR H = 1.

Heating and Magnetic Field	*Density (units of 10^{20} m^{-3})*	*T_E, T_I (KeV)*	ν_{*E}, ν_{*I}	$<\beta>$	$\tau_{E,\,global}$ (msec)	$\tau_{E,\,ISS95}$ (msec)
0.5 MW ECH B = 1 T	0.18	1.4, 0.15	0.02, 1.6	0.7%	16.2	8.1
1 MW ECH B = 0.5 T	0.045	2.1, 0.2	0.002, 0.22	1%	2.1	1.5
1 MW ICH B = 1.0 T	0.83	0.5, 0.5	0.68, 0.64	2%	41.7	11.7
1 MW ICH B = 0.5 T	0.59	0.4, 0.25	0.75, 1.8	3.7%	16.4	5.5

original fixed boundary results. Also, this configuration has been analyzed with the PIES [10] code up to <β> = 1.6%, indicating that only a minimal loss of flux surfaces occurs over the outer 10% of the plasma radius.

3. High <β> Configurations

In addition to the device described in section 2, we have also found nearly quasi–poloidal 2 and 3 field period configurations (R_0/<a> = 2.7 - 3.7) in which the plasma bootstrap current supplies a large fraction of the transform. In the case of 3 field periods, these devices fully access the second regime for ballooning stability at around <β> > 15% with second regime stabilization entering in from the outer region of the plasma at <β> = 6 - 7%. Configurations with 2 field periods have also been found which achieve second regime stabilization for <β>'s as low as 1%. Vertical and external kink modes are weakly unstable at <β> = 15% and can be stabilized by a very small reduction (10%) of the self-consistent bootstrap current. However, these modes are sufficiently near marginal stability that a slight modification in the 3D shape should also provide stabilization. An example of a 3 field period configuration of this type is shown in Figure 3 along with its transform profile with and without plasma bootstrap currents.

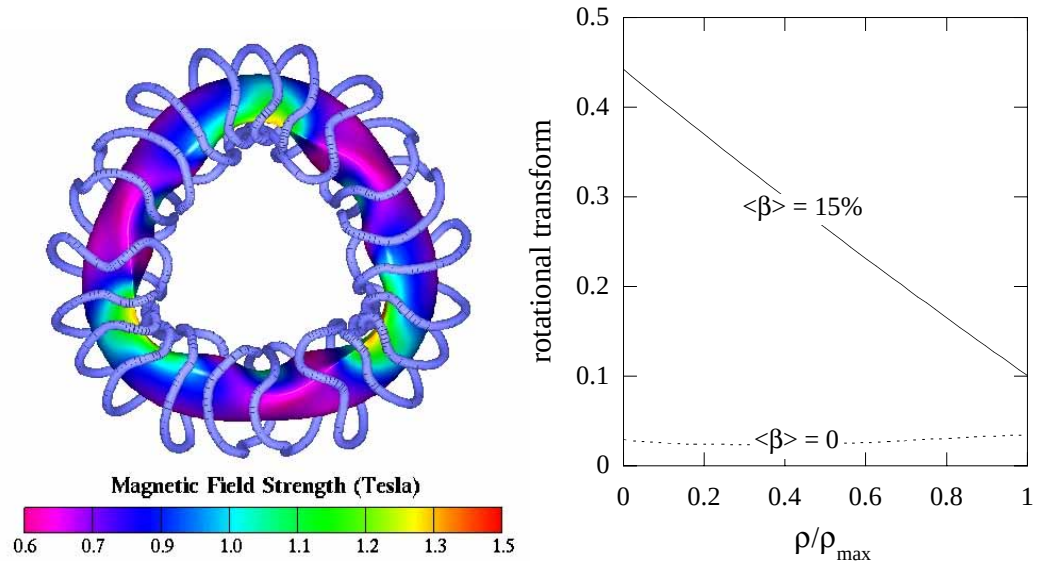

Figure 3 - (a) Top view of outer flux surface with modular coils (in blue) for an N_{fp} = 3, R_0/<a> = 3.7 device; (b) Rotational transform profiles with and without bootstrap current.

At this relatively low value of iota, the collisionless bootstrap current in this device is about 1/4 of that in the equivalent tokamak. These configurations have tokamak-like transform profiles and approach quasi–poloidal symmetry with increasing <β>. This feature is evident in the B_{mn} spectrum shown in Figure 4(a) where the n = 0 [(0,0), (0,1), and (0,2)] components of B_{mn} may be seen to dominate.

At such high values of <β>, the |B| contours also become poloidally closed (at fixed toroidal cross sections) and begin to align with flux surfaces. This is a further indication of the enhancement in quasi–poloidal symmetry associated with increasing <β>. As may be seen from Figure 4(a), the $B_{0,0}$ component is depressed in the center; this is a result of the diamagnetic well (shift due to Pfirsch-Schlüter currents) at this value of <β>. The poloidal gradient B drifts associated with this radial variation in $B_{0,0}$ are helpful for the confinement of

energetic particles, as is shown in the study of alpha confinement in Figure 4(b). Here the curve labeled as the base configuration is constrained to have the same outer flux surface shape and transform profile as the <β> = 23% case, but does not include the plasma diamagnetic current effects which lead to the modified B_{mn} spectrum shown in Fig. 4(a) (i.e., this is essentially a <β> = 0 case, except that an ad-hoc plasma current is provided which is equal to the bootstrap current of the <β> = 23% case). The level of alpha energy losses (~12%) at the highest <β> are the lowest we have found in modeling any of this class of compact stellarator devices.

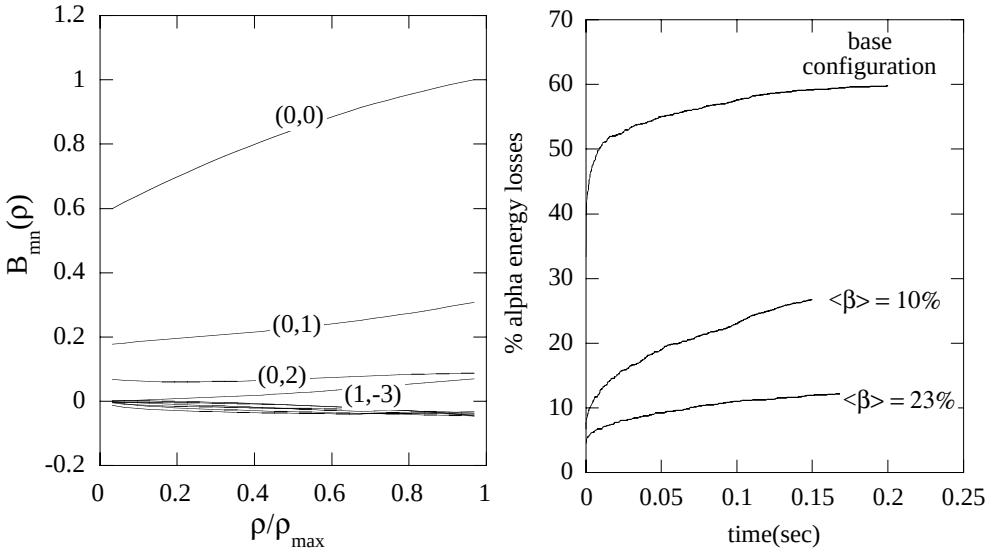

Figure 4 - (a) B_{mn} amplitudes vs. toroidal flux for <β> = 23%, N_{fp} = 3 device, (b) Fraction of 3.5 MeV alpha particle losses for a reactor scale version (R_0 =10 m, <B> = 5 Tesla) with increasing <β>.

4. Conclusions

We have found attractive compact stellarators with 2 and 3 field periods and aspect ratios in the range of $R_0/<a>$ = 2.5 - 3.5 which maintain good neoclassical confinement by approaching quasi-poloidal symmetry. Two classes of this type of compact stellarator have been examined: one which produces most of the rotational transform and quasi-poloidal symmetry through external means and a second which relies more on the plasma currents associated with high plasma <β> to produce these effects.

Acknowledgement - This research was sponsored by the Office of Fusion Energy U. S. Department of Energy, under contract DE-ACO5-00OR22725 with UT-Battelle, LLC, and contract DE-AC020-76-CHO3037 with Princeton Plasma Physics Laboratory.

[1] HIRSHMAN, S.P., SPONG, D.A., WHITSON, J.C., et al., Phys. Plasmas **6** (May, 1999) 1858.
[2] SPONG, D.A., HIRSHMAN, S.P., WHITSON, J.C., et al., Nuclear Fusion **40** (March, 2000) 563.
[3] SANCHEZ,R., HIRSHMAN, S.P., WHITSON, J.C., WARE, A.S., Journal of Comp. Phys. **161** (2000) 576.
[4] SANCHEZ,R., HIRSHMAN, S.P., WARE, A.S., BERRY, L.A., SPONG, D.A.,
Plasma Phys. Contrl. Fusion **42** (2000) 641.
[5] NIELSON, G.H., REIMAN, A.H., et al., Phys. Plasmas **7**, 1911 (2000).
[6] FOWLER, R.H., ROME, J.A., LYON, J.F., Phys. Fluids **28**, 338 (1985).
[7] VAN RIJ, W. I., S. P. HIRSHMAN, Phys. Fluids B1 (March, 1989) 563.
[8] BALDZUHN,J., KICK, M., MAASSBERG, H., W7-AS TEAM, Plasma Phys. Contrl. Fusion **40** (1998) 967.
[9] STROTH, U., et al., Nucl. Fusion **36** (1996) 1063.
[10] REIMAN, A., GREENSIDE, H., Journal of Comput. Phys. **75**, 1423 (1988).